Lawrence Berkeley Laboratory
UNIVERSITY OF CALIFORNIA

Physics, Computer Science & Mathematics Division

Submitted to The Astrophysical Journal

POLARIZATION OF THE COSMIC BACKGROUND RADIATION

Philip M. Lubin and George F. Smoot

August 1980

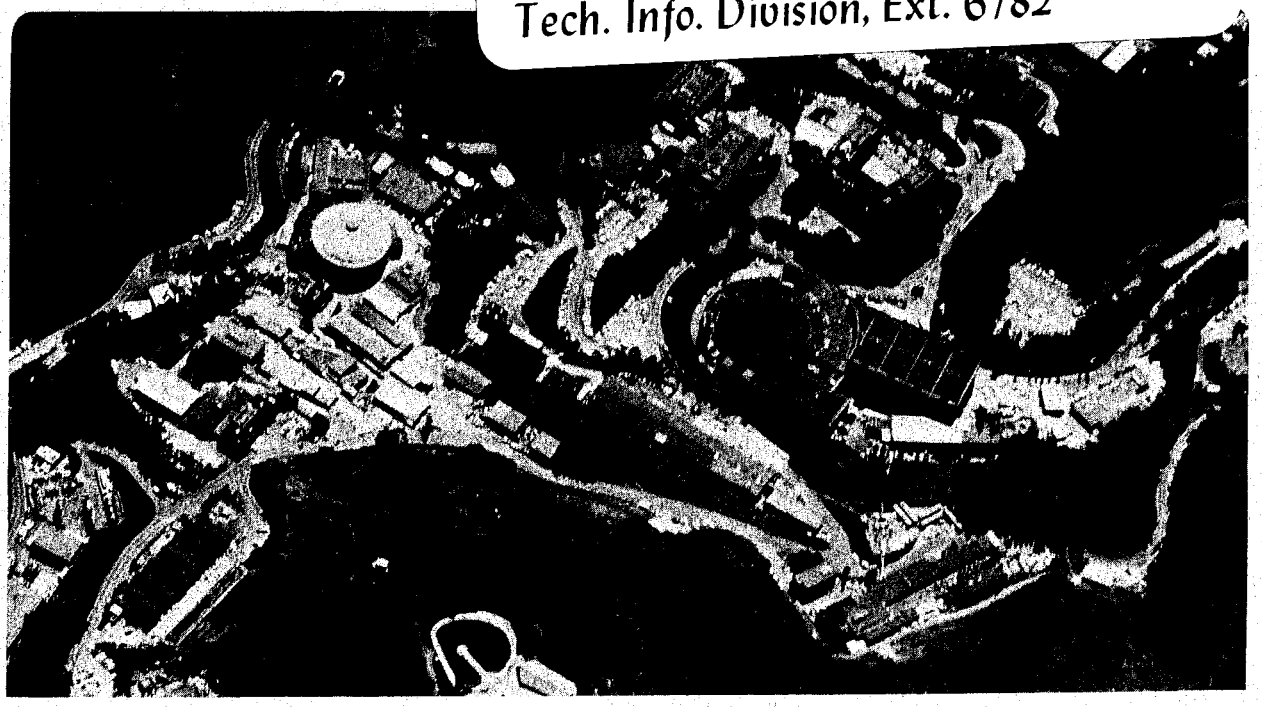

Prepared for the U.S. Department of Energy under Contract W-7405-ENG-48

Subject heading: Cosmic Background Radiation, Cosmology.

POLARIZATION OF THE COSMIC BACKGROUND RADIATION

Philip M. Lubin and George F. Smoot

Space Sciences Laboratory and Lawrence Berkeley Laboratory

University of California at Berkeley

Berkeley, California 94720

ABSTRACT

We discuss the technique and results of a measurement of the linear polarization of the Cosmic Background Radiation. Data taken between May 1978 and February 1980 from both the northern hemisphere (Berkeley Lat. 38°N) and the southern hemisphere (Lima Lat. 12°S) over 11 declinations from -37^{o} to $+63^{o}$ show the radiation to be essentially unpolarized over all areas surveyed. Fitting all data gives the 95% confidence level limit on a linearly polarized component of 0.3 mK for spherical harmonics through third order. A fit of all data to the anisotropic axisymmetric model of Rees (1968) yields a 95% confidence level limit of 0.15 mK for the magnitude of the polarized component. Constraints on various cosmological models are discussed in light of these limits.

1. INTRODUCTION

The cosmic background radiation, discovered by Penzias and Wilson (1965), has profoundly influenced our understanding of the universe: it is thought to be the relic radiation of the primordial fireball, emitted within minutes of the Big Bang. The study of this radiation is a unique probe into the structure of the universe.

The cosmic background radiation field can be characterized at a fixed point in space in terms of its

(1) Spectrum $\vec{E}(\vec{\kappa}, \omega)$,

(2) Angular distribution $\vec{E}(\vec{\kappa}, \omega)$, and

(3) Polarization state $\vec{E}(\vec{\kappa}, \omega)$.

Our current understanding of the spectrum is that it is essentially a blackbody with a characteristic temperature about 3 K with a possible deviation ($\approx$15%) near the peak (Woody and Richards, 1979). The angular distribution of the radiation is nearly isotropic with a deviation of amplitude $\sim$ 3 mK (0.1%) interpreted as being due to the motion of the earth through the radiation field (Corey and Wilkinson, 1976; Smoot, Gorenstein, and Muller, 1977). After removal of this "first order anisotropy" no residual anisotropy is seen with a 95% confidence level of 1 mK for quadrupole terms (Cheng *et al.*, 1979; Smoot and Lubin, 1979; Gorenstein and Smoot, 1980) except for a recent report by Fabbri *et al.* (1980) of a possible quadrupole component at the level of $0.9^{+\ 0.4}_{-\ 0.2}$ *mK*. As they indicate, this is tentative because of the limited sky coverage their experiment had.

Although Rees (1968) suggested that anisotropic expansion of the universe could yield a net linear polarization in the cosmic background radiation, little attention has been directed towards using polarization measurements to search for anisotropies. In 1972, George Nanos (1974, 1979), under Dave Wilkinson at Princeton, initiated an experiment to search for linear polarization with a null result. In addition, Caderni *et al.* (1978a) reported no net linear polarization from a balloon-borne infrared experiment. Unfortunately the balloon flight was ter-

minated prematurely, and only a small portion of the sky was surveyed. Table 1 summarizes the previous measurements.

Table 1
Measured Limits on Linear Polarization 95% Confidence Level

Reference	Wavelength (cm)	Sky Coverage	Limit
Penzias and Wilson (1965)	7.35	scattered	10%
Nanos (1974, 1979)	3.2	declination = +40°	0.06%
Caderni *et al.* (1978)	0.05 - 0.3	near galactic center	0.1 - 1%
Lubin and Smoot (1979)	0.91	declinations 38° , 53° , 63°	0.03%
This work	0.91	11 declinations -37° to +63°	0.006%

Anisotropies

There are two basic classes of anisotropies: those intrinsic to the radiation and those extrinsic in origin. The extrinsic anisotropies are typified by the first order anisotropy caused by the motion of the observer through the radiation.

If an intrinsic intensity anisotropy exists in the cosmic background radiation, then the radiation can acquire a net linear polarization by Thomson scattering from electrons in ionized matter. *Any intrinsic anisotropy is therefore accompanied by a net polarization, if the anisotropy originated before the period of recombination.* Extrinsic types of anisotropies are generally not accompanied by a net polarization. Table 2 gives those types of anisotropies expected to produce polarization.

In general, intrinsic anisotropies are expected to exist, although their level is uncertain. From causality arguments, anisotropies should arise because widely separated parts of the universe have always been out of communication with other parts. In simple models, anisotropy is expected on an angular scale size characterized by $\theta_c = 4.2^o\sqrt{q_o}$ where q_o is the deceleration parameter (Weinberg, 1972). If $q_o = 0.5$ (minimum needed for closed universe), then $\theta_c = 3^o$. Anisotropic expansion of the universe causes an anisotropy because the universe expands more rapidly in some directions than in others, and thus radiation is red shifted by

Table 2. Possible causes of polarization and anisotropy in the 3K cosmic background radiation.

POSSIBLE CAUSES OF ANISOTROPY AND POLARIZATION IN THE 3 K COSMIC BACKGROUND RADIATION

ANISOTROPY CAUSE	*TYPE*	*POLARIZATION*
Motion of observer	LOCAL	NO
Rotation of universe	INTRINSIC	YES
Long wavelength gravity waves	INTRINSIC	YES
Anisotropic expansion (Shear)	INTRINSIC	YES
Density inhomogeneities		
A) Primordial	INTRINSIC	YES
B) Local	LOCAL	NO
Motion of source	INTRINSIC	YES
Transverse motion of clusters	LOCAL	YES

differing amounts in different directions. Figure 1 shows the polarization pattern expected for two cases of an axisymmetric expansion. If the universe were rotating, then an intrinsic anisotropy would also be expected (Hawking, 1969). Anisotropy measurements and therefore polarization measurements provide a test of Mach's principle (Mach, 1893).

Studying the polarization properties of the radiation serves a dual purpose: it measures possible inherent polarization that may exist while being insensitive to local causes of anisotropy such as our motion, and it provides a secondary means of searching for any intrinsic anisotropy in intensity. In addition, the discovery of both intensity and polarization anisotropies and a measurement of their relative magnitudes provides information about the intergalactic medium.

Polarization measurements also provide a check of the first order anisotropy seen in intensity. If the anisotropy is due to our motion, no net polarization is expected; however, if this first order anisotropy is intrinsic to the radiation itself, in part or in total, a net polarization could exist. So a null result tends to support the interpretation of the intensity anisotropy as being locally induced by our motion.

Figure 1. Expansion anisotropy and resulting polarization pattern on the sky for two simple axisymmetric anisotropic models.

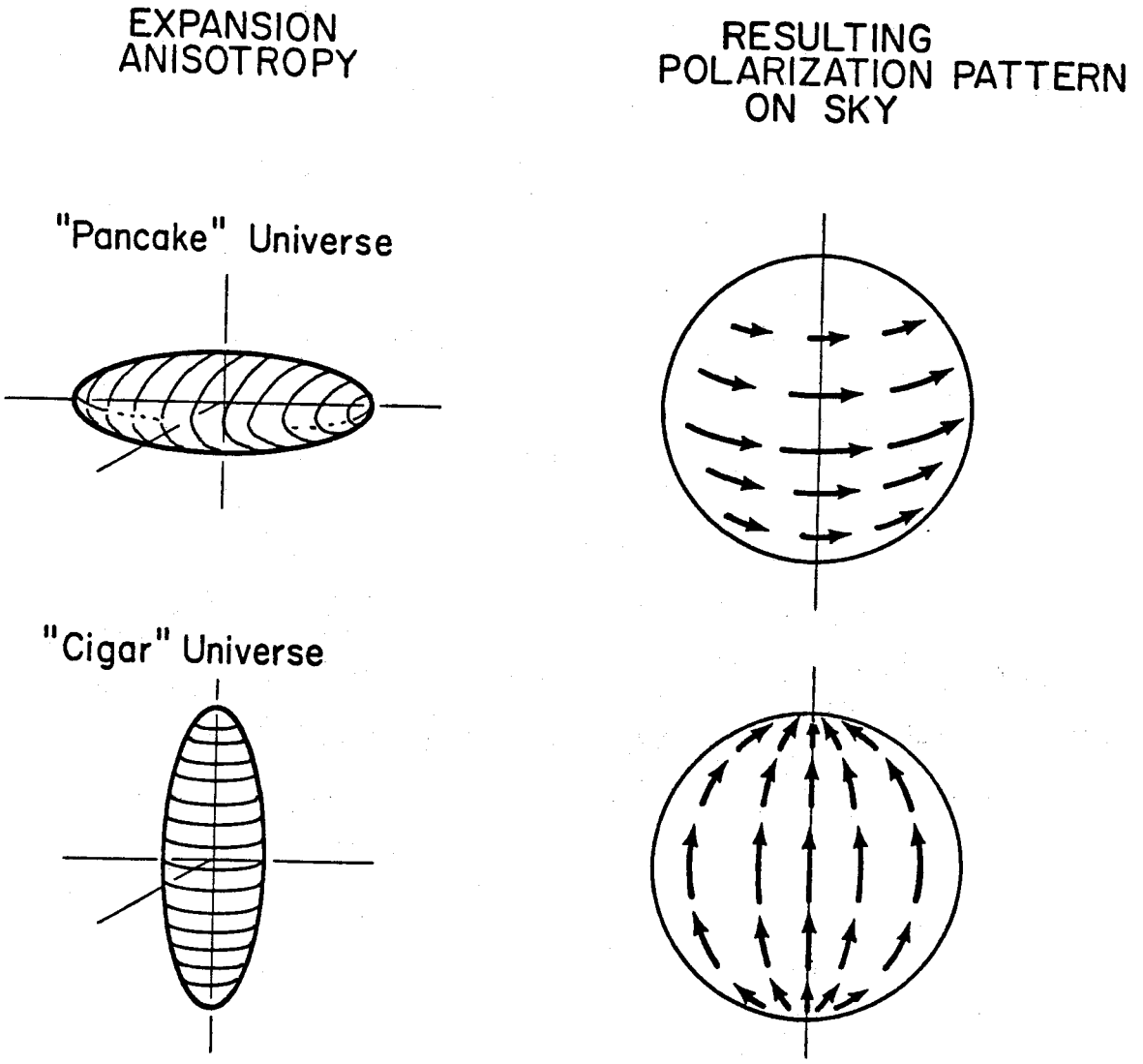

2. ANTENNA TEMPERATURE AND STOKES PARAMETERS

The experiment has been designed to measure the Stokes parameters of linear polarization Q and U for the Cosmic Background Radiation.

For blackbody radiation of temperature T, the flux I is given by:

$$I = \frac{2h\nu^3}{c^2} \frac{1}{e^{h\nu/kT}-1} \quad erg\ cm^{-2}\ sec^{-1}\ st^{-1}\ H_z^{-1} \tag{1}$$

for hν << kT (the Rayleigh-Jeans limit). This reduces to:

$$I = \frac{2kT}{\lambda^2}. \tag{2}$$

For a given flux I (ergs cm^{-2} sec^{-1} st^{-1} Hz^{-1}), the antenna temperature T_A is defined such that, in the Rayleigh-Jeans limit, the flux produced by a blackbody of temperature T_A would produce the given flux I. Because microwave radiometers measure flux, it is convenient to define an equivalent temperature T_A as:

$$T_A = \frac{\lambda^2}{2k} I. \tag{3}$$

Using (1) for I gives:

$$T_A = \frac{x}{e^x-1} T, \quad x = \frac{h\nu}{kT}. \tag{4}$$

Also

$$\frac{dT_A}{dT} = \frac{x^2e^x}{(e^x-1)^2}. \tag{5}$$

The antenna temperature at ν = 33 GHz for T = 2.7 K is:

$$T_A = 2.0\ K \quad while \quad \frac{dT_A}{dT} = 0.98. \tag{6}$$

In terms of antenna temperature Q and U are defined as follows:

$$Q = T_{NS} - T_{EW} \tag{7}$$

$$U = T_{NW,SE} - T_{NE,SW} \tag{8}$$

where:

T_{NS} = antenna temperature of radiation polarized along the north-south direction

T_{EW} = antenna temperature of radiation polarized along the east-west direction

$T_{NW,SE}$ = antenna temperature of radiation polarized along the northwest-southeast direction

$T_{NE,SW}$ = antenna temperature of radiation polarized along the northeast-southwest direction

Stokes parameters are ideally suited for this experiment since the measured quantities differ from the Stokes parameters by a simple scale factor.

If the measuring instrument is initially aligned to measure Q, rotation of the instrument by 45^o gives U, while a rotation by 90^o reverses the sign of the measured parameter. Most instrumental effects are either constant with rotation or change sign under rotation by 180^o. Rotating in 45^o increments through a full 360^o will therefore measure Q and U as well as the instrumental effects. This is a crucial aspect of the experiment, since we are attempting to measure polarization to a level which is one-hundredth of the instrumental effect and one-ten-thousandth of the intensity of the cosmic background radiation.

3. EXPERIMENTAL APPARATUS AND PROCEDURES

The apparatus is shown schematically in Figure 2. The 9.1 mm Dicke radiometer uses a Faraday rotation switch to switch between polarization states. The antenna axis can tilt relative to vertical in order to observe various declinations from a fixed latitude. The ground shield aids in rejecting radiation from nearby objects. A stepping motor rotates the radiometer about its axis to allow both Stokes parameters Q and U to be measured and to provide a basic symmetry in order to cancel instrumental effects. A rain shield of 0.5 mil polyvinylidene (Saran Wrap) provides protection from rain and dust.

a) Microwave Radiometer

The radiometer includes a superheterodyne microwave receiver operating at 9.1 mm wavelength which is rapidly switched between two orthogonal polarization states, giving an output voltage proportional to the power difference in these two polarization states. As with all receivers, the instrument has a sensitivity limited by its intrinsic noise. The rms output temperature fluctuations ΔT, measured by a square-wave switched, narrow-band detected radiometer, are $\Delta T = \frac{2.2 T_{sys}}{\sqrt{B\tau}}$, where T_{sys} is the system noise temperature (characteristic of system performance), B is the IF bandwidth, and τ is the measurement time (Kraus, 1966). For our instrument, the system noise temperature is typically T_{sys} = 520 K and the IF bandwidth is B = 500 MHz, so ΔT = 52 mK $sec^{-1/2}$. Thus, by measuring for a sufficient period of time the desired sensitivity can be obtained. For example, a one year integration provides a theoretical sensitivity of 0.01 mK.

The radiometer is encased in a metal can which provides RF shielding. The radiometer is electrically insulated from the can, decoupling any possible grounding effects. The lockin amplifier uses an "ideal" integrator and a narrow band amplifier, (Q = 10), with a center frequency of 100 Hz, and it responds only to signals synchronous with the switching of the Faraday rotation switch. The output of the lockin is digitized and recorded on a remote tape

Figure 2. Schematic of microwave polarimeter used.

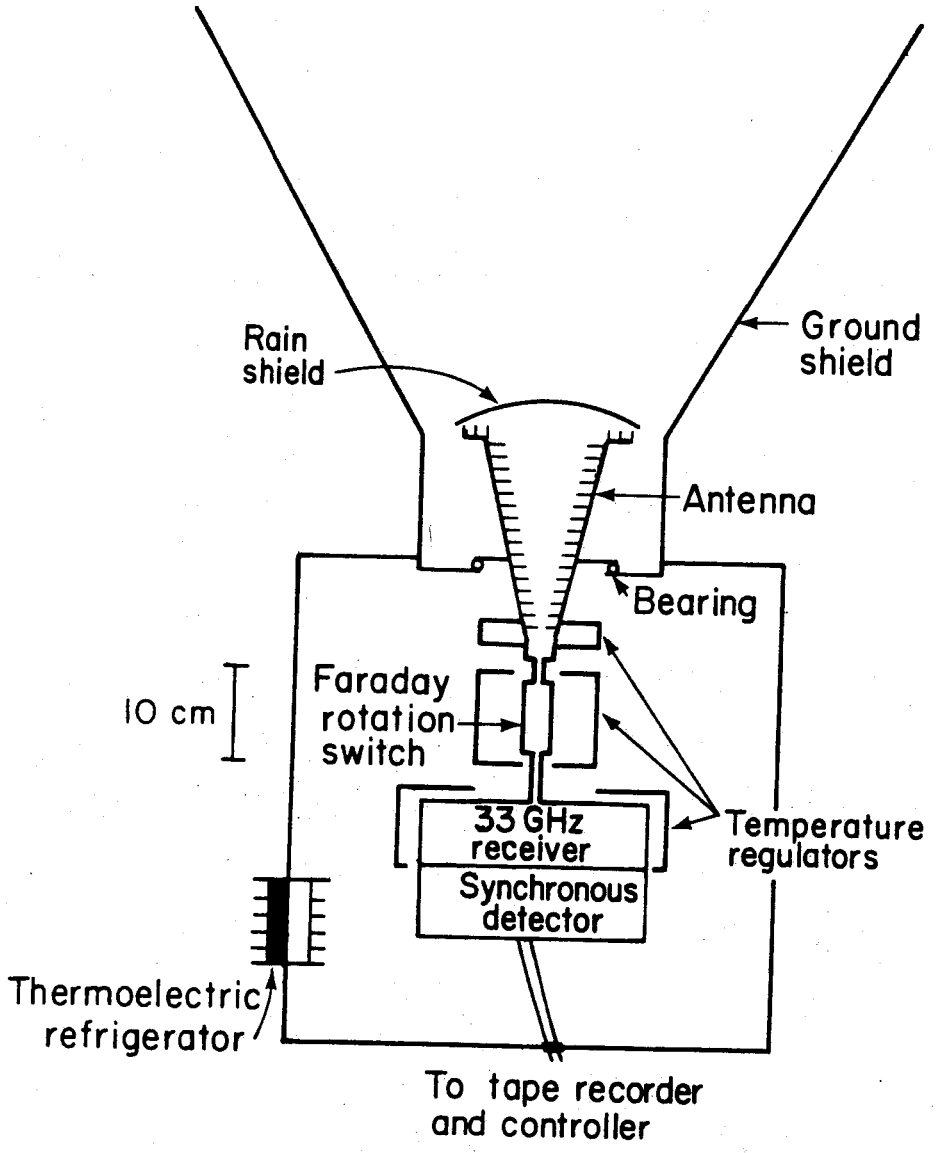

XBL 7910-4283A

recorder. Because the distance from radiometer to tape is typically 100 feet or more, a shielded twisted-pair line driver-receiver system is used to transmit and receive the data. This has the added virtue of eliminating any ground loops between the tape recorder and radiometer.

b) Thermal Regulation

Thermal regulation of the instrument is crucial because the various components, particularly the Faraday rotation switch, are sensitive to temperature variations. As shown in Figure 2, we thermally regulate three sections: the lower portion (throat) of the antenna, the Faraday rotation switch, and the microwave receiver. In addition, the lockin amplifier is temperature stabilized through attachment to the regulated receiver block of the receiver.

Regulation is achieved by a combination of active and passive thermal elements. The three regulated areas have independent linear proportional heaters with feedback from sensors at the critical points, achieving a typical thermal regulation of ± 0.2 C. Large thermal capacity in the form of aluminum blocks assures that heat is evenly distributed with a long time constant so that the time-rate of change of the temperature is less than 0.3 C per hour. An analysis of the temperature stability of the components, shows that the temperature changes cause less than 0.06 mK error in Q and U (Lubin , 1980a). A thermoelectric refrigerator insures that regulation is achieved even during periods of warm weather.

c) Calibration

Calibration is periodically performed using a polarized blackbody source at ambient temperature. The calibrator is shown in Figure 3. Theoretical calculations (Chu, Gans, and Legg, 1975) and our own radiometric measurements show that the calibrator is nearly ideal in that the polarized signal is equal to the difference in temperature between the polarized reference blackbody (eccosorb) and the sky.

The wire grid in the calibrator is made of photo-etched copper-plated 2 mil Kapton. The wires are spaced 0.64 mm on center. This dimension is not critical as long as it is small

Figure 3. Sketch of polarized calibrator used.

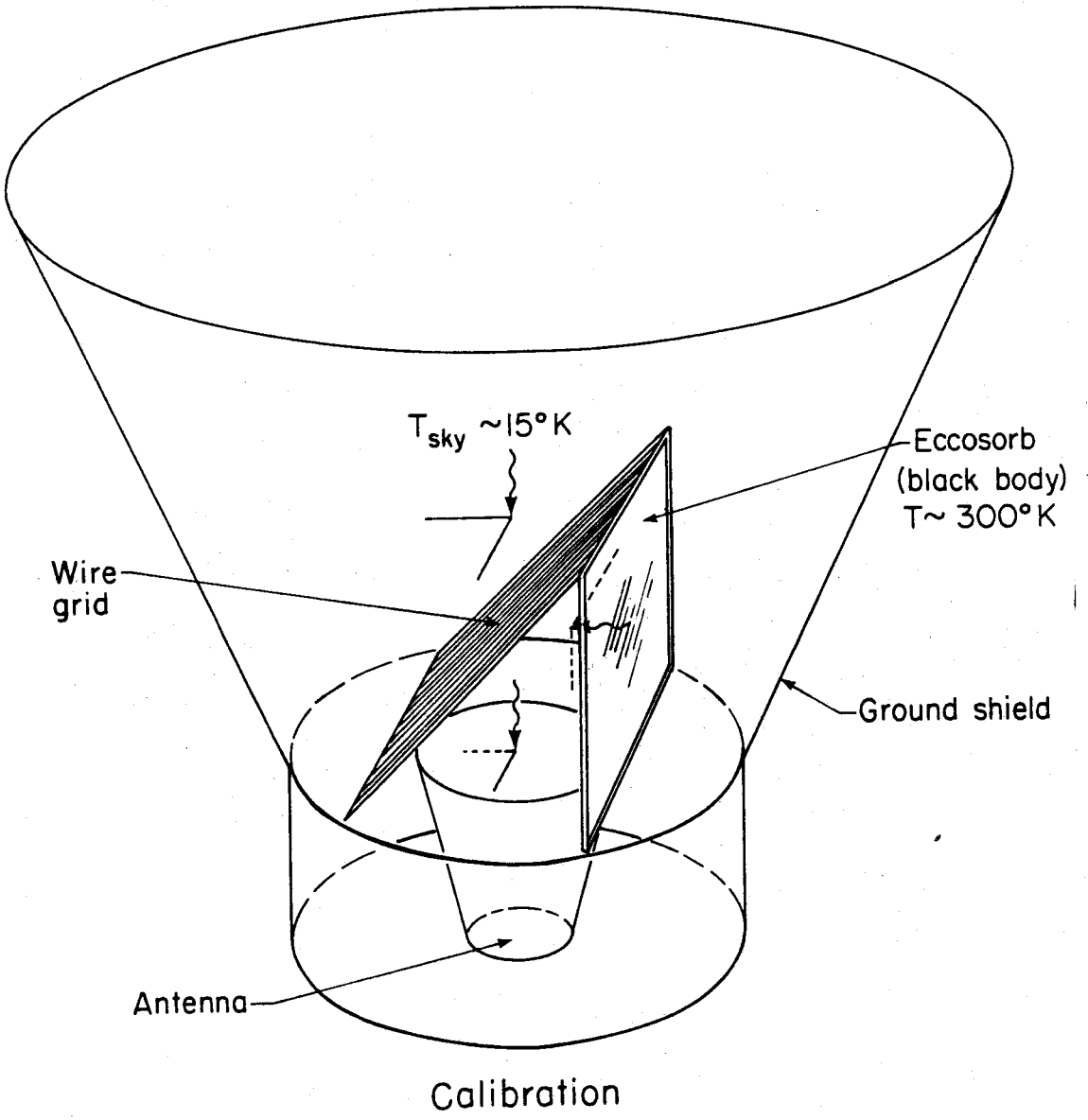

compared to the wavelength of 9.1 mm. The grid is canted at a 45° angle. Radiation whose electric field (polarization) is along the wire direction will be reflected, whereas radiation polarized perpendicularly will be transmitted. This is precisely analogous to the optical case of a Polaroid sheet, where the conductive wires are provided by iodine ions on a stretched polymer grid (Shurcliff and Ballard, 1962).

The calibration signal seen by the polarimeter is a partially polarized signal, the magnitude of the polarized part being the difference in temperature between the eccosorb (ambient temperature blackbody source) and the sky (atmosphere plus background radiation). Independent measurements of the atmospheric contribution give $T_A \sim 12 \pm 1\ K$ for a typical clear day. The presence of variable amounts of water vapor can change this by several degrees Kelvin. Adding the 2 K contribution of the cosmic background radiation yields a sky temperature of $T_A = 14\ ^{+\ 4}_{-\ 1}\ K$ where the skewed error is due to the variability of water vapor in the atmosphere.

Independent radiometric measurements at 33 GHz give an insertion loss through the grid of 1.5 ± 0.1% for the transmission mode and reflection of 99 ± 1% in the reflection mode. The eccosorb temperature is measured for each calibration with an error of less than 1%. The total polarized signal is then $T_{cal} = T_{ecc} - 14\ K$ with an error of less than 4%. An additional calibration using the same receiver, but replacing the Faraday rotation switch with a Dicke switch, is in agreement to within 5%.

d) Data Acquisition

The radiometer signal is integrated for 100 seconds, after which it is digitized with 12 bit resolution and recorded. The radiometer is rotated by 45°, and the process is repeated until a 315° rotation has been achieved. The instrument then rotates back to its 0° initial position and the cycle repeats. The system is automated and runs unattended except for cleaning and occasional repair.

A typical tape records about two weeks of data before being analyzed. After the analysis this data is added to a library tape containing all previous data. Time is recorded from a crystal controlled clock for later binning of data and correlation of time related events. The basic record structure consists of eight 40 byte elements corresponding to a full rotation cycle. Each data element corresponds to a rotation position and consists of the signal, time, rotation position, and various housekeeping signals. Each full record contains all the information necessary to calculate the Stokes parameters. Data taken during periods of rain or dew are deleted and the humidity is recorded, allowing an additional check of contaminated data.

The northern declination data are taken from the Lawrence Berkeley Laboratory, at a latitude of 38°N. During periods of rain the equipment is either removed or covered. Southern declination data were taken from the Naval Air Base at the Jorge Chavez airport in Lima, Peru, latitude 12°S during March, 1979. These measurements were made along with our U-2 experiment to measure the intensity anisotropy. Although heat, dust, power failures, and logistics made the southern data-taking less than optimal, useful data were obtained.

In both hemispheres the instrument was aligned along the north-south direction so that Q and U were properly defined. The instrument is always tilted along the north-south direction, so that as the earth sweeps the antenna beam along a constant declination the proper orientation of Q and U is maintained. During a typical run the instrument was pointed towards a fixed declination for two weeks with a calibration at the beginning and the end of the run. Multiple runs are taken at most declinations. Figure 4 shows the sky coverage obtained from both the

Figure 4. Shaded areas show sky coverage achieved in the experiment. Northern declination scans were taken from Berkeley while the southern declination scans were made from Lima, Peru.

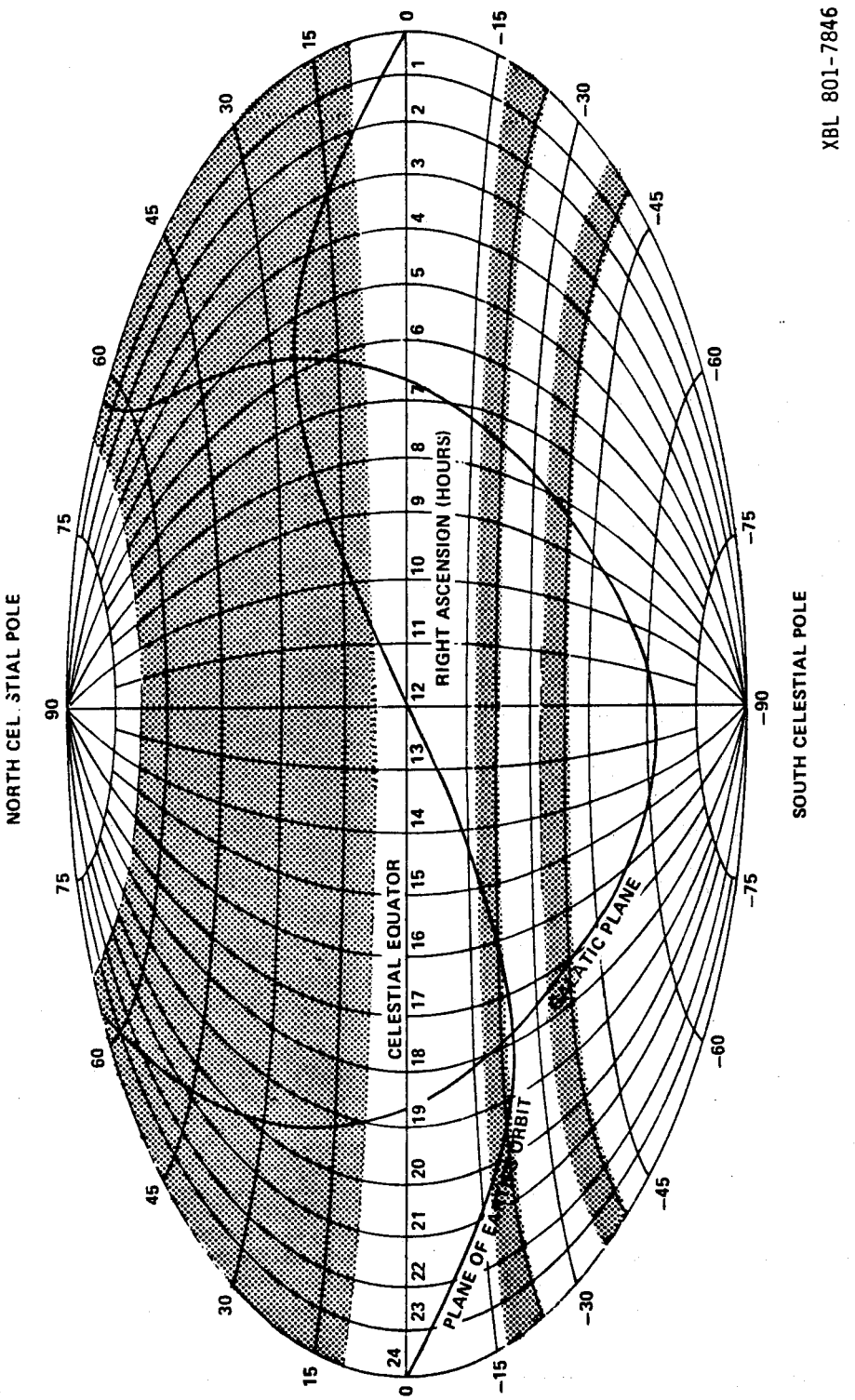

northern and southern hemisphere. In total, eleven declinations were surveyed ranging from -37^o to $+63^o$ declination.

e) Wobble Correction

When the instrument is tilted away from the local vertical, the gravitational torque on the radiometer causes stress on the components. This leads to a modulated offset with the same period as the instrumental rotation. A true polarized signal would have a period which is one half of the rotation period. Rotation by a full 360^o cycle in 45^o steps would appear to allow complete cancellation of this effect. However, there is a residual second order effect at the one percent level, apparently caused by the mechanical asymmetry of construction, which adds a constant term to both Q and U. The mechanical nature of this wobble was verified by physically rotating the instrument by 180^o and noting that the DC (average) level of Q and U reversed sign.

For the northern hemisphere runs, the typical wobble correction is a few tenths of a milliKelvin. During the southern hemisphere measurements, the instrument was in a different configuration. In addition, a bolt worked loose during data taking at $\delta = -37^o$, causing a false polarized signal of about a milliKelvin. The errors for the $\delta = -37^o$ data were increased in an effort to allow for the possible systematic errors caused by the larger wobble. It is important to note that this correction is only to the average level and does not affect the time dependence of the data. For the 38° declination data where there is essentially no wobble correction, the DC (average) level is consistent with zero, $10 \pm 60\ \mu$K for Q and $30 \pm 60\ \mu$K for U.

To make the correction, the northern and southern hemisphere data are analyzed separately. A least-squares fit is made to the wobble versus DC level, assuming a linear relationship and forcing the fit through the origin. The fit is made separately for Q and U in the northern hemisphere runs. A linear relationship is expected because of the mechanical nature of the effect. The data and best fit are shown in Figure 5.

Figure 5. Average value of Stokes parameters Q and U versus instrument wobble amplitude for other than vertical looking runs.

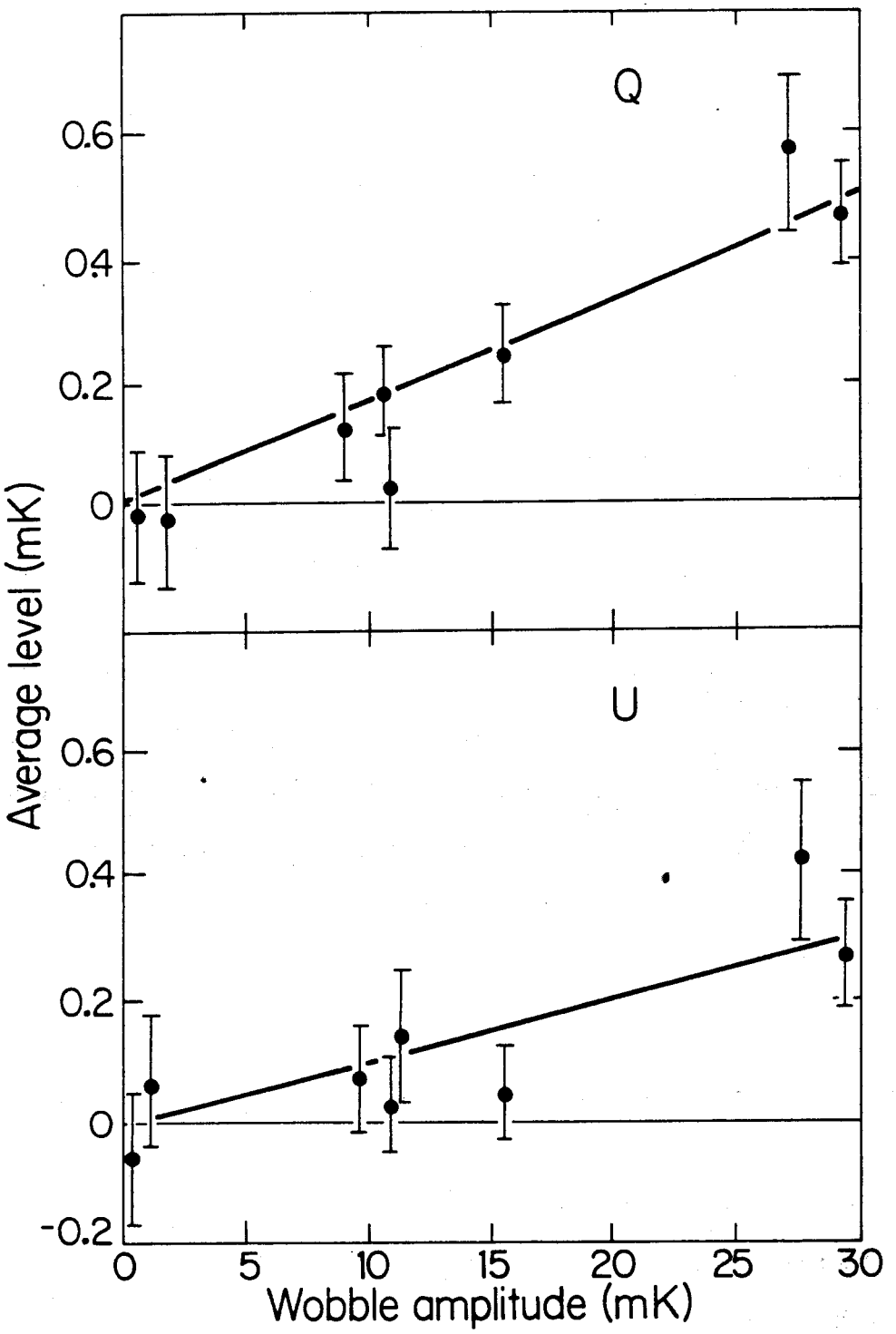

f) Data Reduction

To eliminate the instrumental offset (average DC output) and to obtain both components of linear polarization, the instrument is rotated in 45^o increments about the horn axis.

A basic rotation cycle produces eight values $S_1,...,S_8$, corresponding to rotation positions 0^o, 45^o, ... 315^o. The offset is constant with rotation angle (except for the wobble which changes sign under rotation by 180^o, while any signal indicative of a true polarization would reverse sign upon rotation of the instrument by 90^o. Q and U can thus be calculated as follows:

$$Q = (S_1 - S_3 + S_5 - S_7)/4 \tag{9}$$

$$U = (S_2 - S_4 + S_6 - S_8)/4 \tag{10}$$

The offset is calculated as the average of $S_1,...,S_8$.

Sidereal time is calculated for each value of Q and U from the recorded universal time. A least-squares fit is made to Fourier components with periods of DC (constant) 24, 12, 8, 6, and 4.8 hours for Q and U at each declination observed. Q and U are binned in hourly sidereal bins and time plots are made. Global fits are constructed by making a least-squares fit to the hourly bins at each declination, using a series of spherical harmonics as fitting functions.

g) Data Deletion

Deleted or edited data fall into two categories: data which can be eliminated because of known causes (sun overhead, rain, cleaning ground shield), and data which have obvious non-statistical behavior of unknown origin. The latter category is somewhat more difficult to quantify in terms of a rejection threshold. Our philosophy is to use all data which are not "obviously" bad, so as not to bias the results.

A diagnostic program is run on the data to test their statistical properties. Table 3 lists the statistical tests performed.

In theory, the minimum detectable signal is inversely proportional to the square root of

Table 3 Statistical Tests of Data Performed	
Fourier Transform	Test for Spurious Periodic Signals
Run Test	Test for Random Nature of Data Above and Below Mean
Gaussian Statistics	Check for Gaussian Nature of Data and look for Non-statistical Behavior in Tails of Distribution
Integration Test	Check for low level systematic errors by plotting RMS fluctuations of binned data against number of data points in each bin. The fluctuations should average down inversely as the square root of the number of data points in each bin.

the integration time. This integration test is of particular importance, as it tells us whether or not the data "integrates down" properly. The test is included in the diagnostic program and a sample is shown in Figure 6. The $\frac{1}{\sqrt{N}}$ line is drawn in for comparison.

Figure 6. RMS fluctuations versus integration time. $1/t^{\frac{1}{2}}$ line is drawn in for comparison.

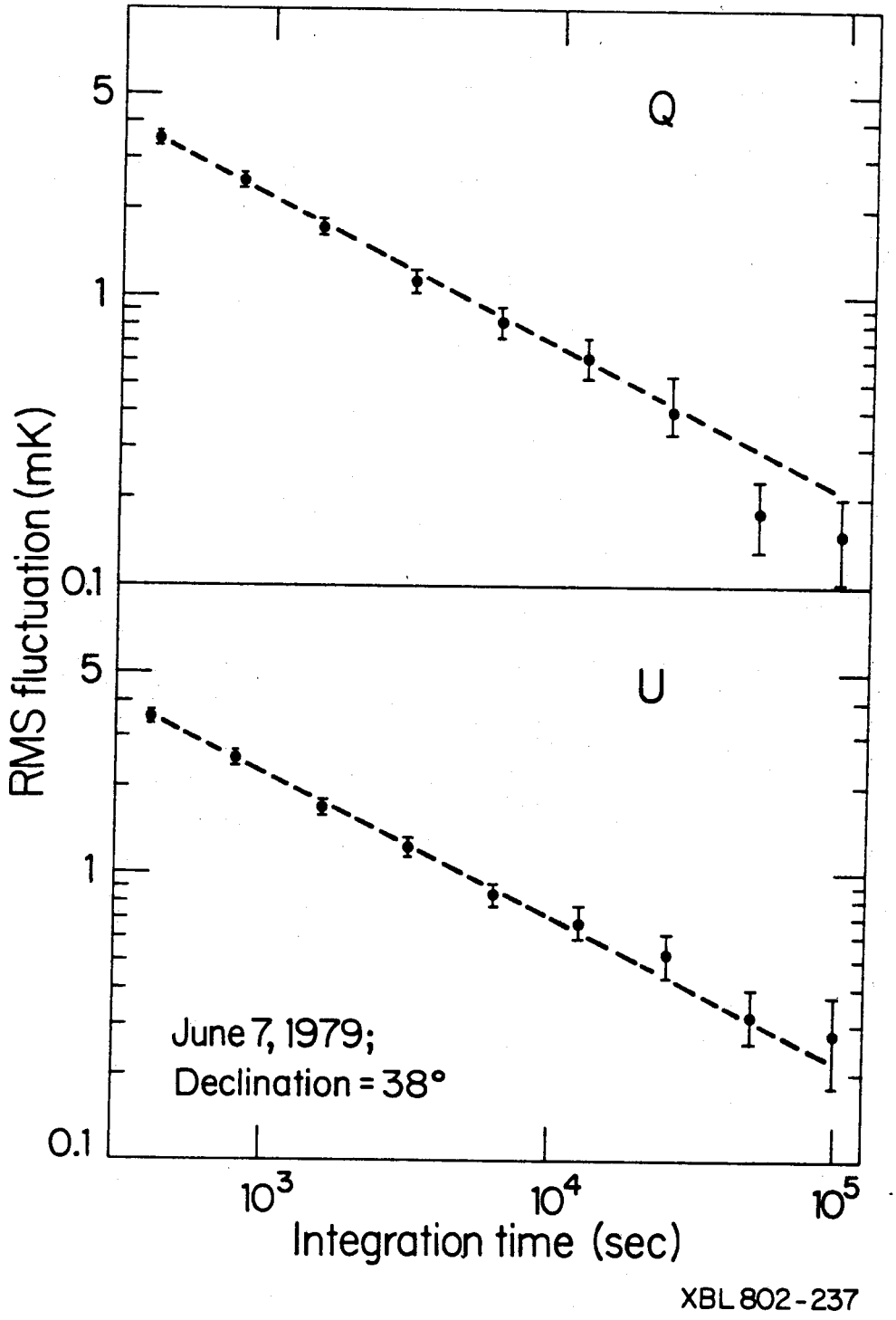

There are two approaches in dealing with extraneous backgrounds: either subtract the background emission in the data analysis, or design the experiment to avoid or eliminate the backgrounds. We have adopted the latter philosophy.

a) Galactic and Extragalactic

Diffuse galactic emission is dominated by synchrotron radiation and emission from ionized hydrogen (HII). Synchrotron emission is typically 10-50% linearly polarized, while HII emission is not. Synchrotron emission is thus more relevant as a background. Figure 7 gives an estimate of the total synchrotron emission at 33 GHz based on low frequency surveys (Witebsky, 1978). Surveys at low frequency have been made which measure the polarization (Berkhuijsen, 1971, 1972; Brouw and Spoelstra, 1976). Utilizing the 1411 MHz polarization survey of Brouw and Spoelstra, the polarized emission at 33 GHz was estimated. Figure 8 shows a contour map estimation of the total polarized signal based on their data. The extrapolation assumes $T_A \sim \nu^{-2.8}$ with errors likely to be no more than a factor of two. Because the beam pattern of the antenna is fairly broad, extragalactic sources are negligible at the 0.1 mK level for all known sources.

b) Earth

The earth is a strong source of thermal microwave radiation, and if viewed directly, would have an antenna temperature of 300 K. This radiation is unpolarized, but the slightly asymmetric antenna response with polarization could result in an apparent signal from the earth. The measured antenna pattern convolved with the theoretical diffraction past the conical ground shield predicts that the apparent signal from the earth should be less than 0.1 mK for vertical data, and less than 0.2 mK when the apparatus is tilted by 25°, which was the maximum tilt angle used. This apparent signal should be essentially constant, since the temperature and

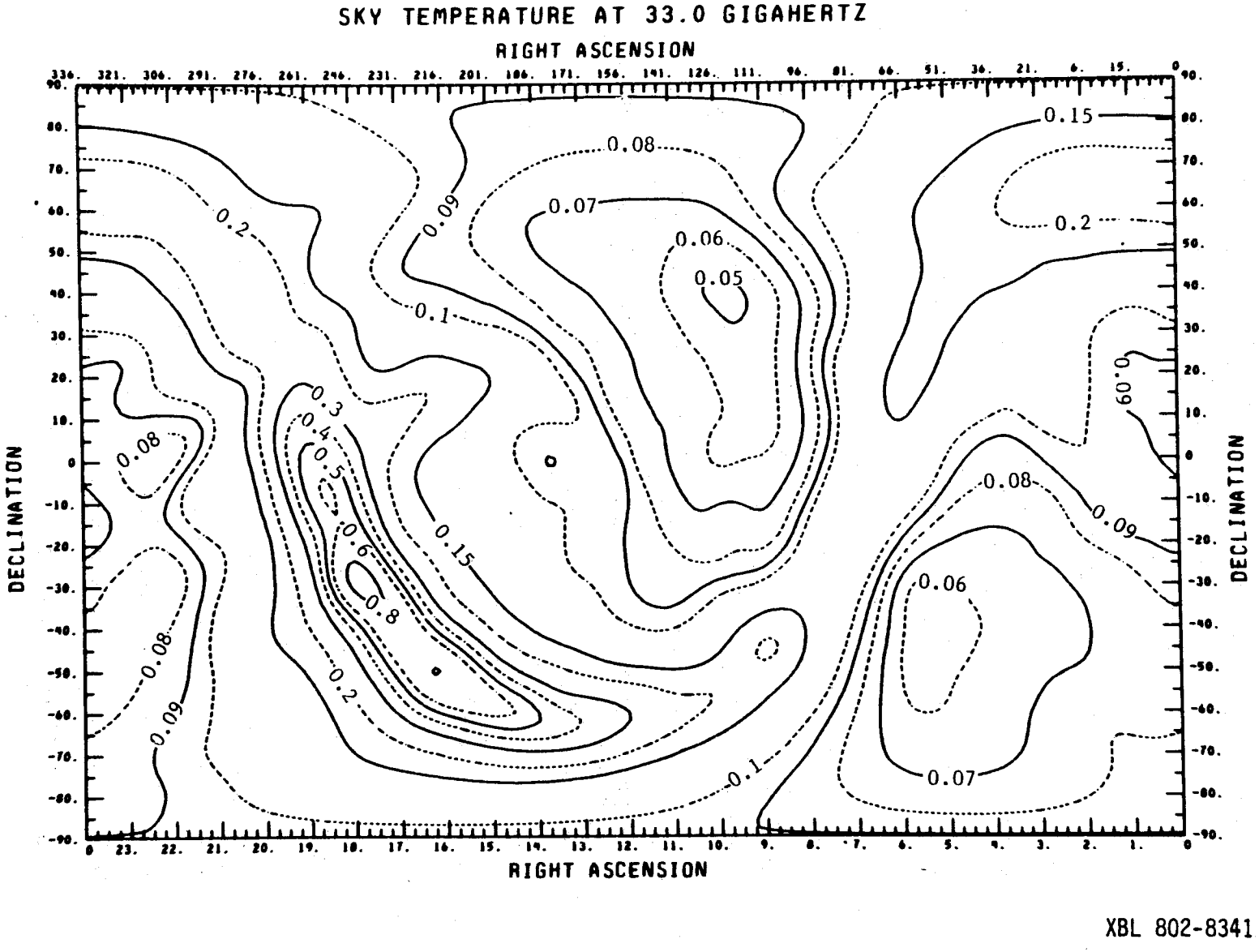

Figure 7. Contour map of total estimated galactic synchrotron emission at 33 GHz obtained from lower frequency measurements. Levels are in milliKelvins.

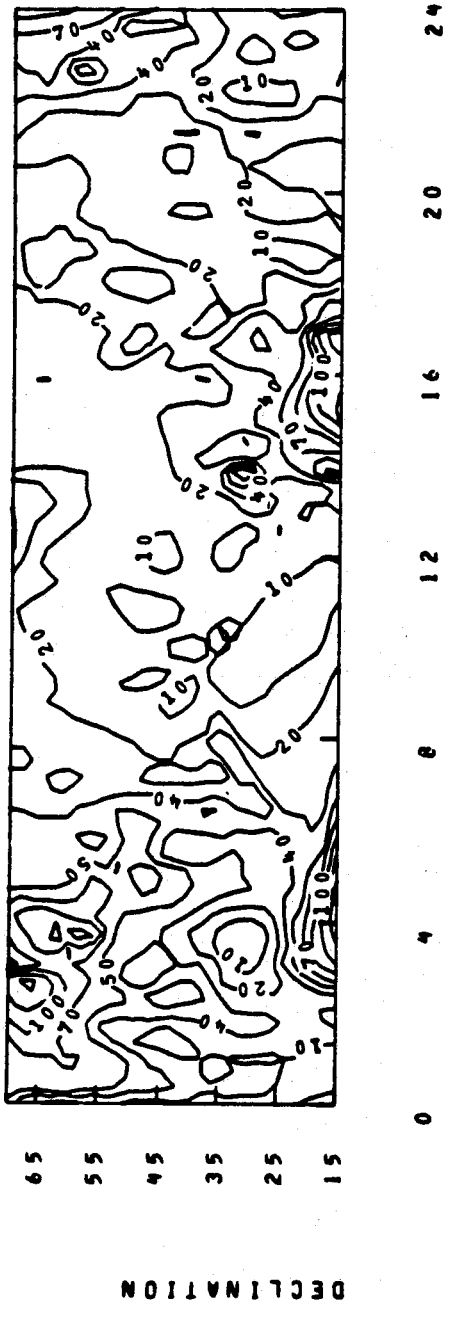

XBL 802-8340

Figure 8. Contour map of estimated polarized galactic synchrotron emission at 33 GHz based upon the survey of Brouw and Spoelstra (1976). Levels are in microKelvin.

hence emission from the earth typically varies less than 3% during a 24 hour period.

We performed a test of the sidelobe and diffraction calculation by tilting the apparatus northward 25^o toward a hill rising about 8^o above the horizon and then erecting a large ground shield. The results of this test show that the earth in the antenna sidelobes contributes no more than 0.24 ± 0.17 mK in this extreme case. We expect that for most of the data the earth-contributed signal is much lower than the limit set for this large tilt and is therefore negligible.

c) Solar System Sources

The sun and moon are a potential background, because small differences in the antenna response pattern to differing polarization states of powerful unpolarized sources can produce small signals in the instrument. For this reason data are ignored when these objects are close to the beam axis. The induced signal is less than 0.1 mK when the sun is more than 30^o from the beam axis, while the corresponding angle for the moon is 20^o.

d) Satellites

A satellite broadcasting at 33 GHz would present a serious background. Fortunately, technology has not progressed to this point, although in several more years this may no longer be the case. A list of broadcasting sources from ECAC (Electromagnetic Compatibility Analysis Center) in Annapolis, Maryland shows that we are relatively safe from this type of manmade radiation.

e) Dust

Solar system (zodiacal) and galactic dust do not produce significant polarized signals at our observing frequency. Infared balloon-borne measurements indicate that the total intensity should be well below 0.1 mK everywhere except in certain isolated regions near the galactic plane (Owens *et al.*, 1979). The polarized component would be substantially less.

f) Atmosphere

The atmosphere has an equivalent antenna temperature of about $T_A = 12\ K$. Fortunately, the emission is not significantly polarized at our frequency. Fog does not appear to be a problem except when it condenses on the rain shield, and data taken during periods of heavy fog or rain are eliminated. Although scattered sunlight is significantly polarized at optical wavelengths, very little is scattered in the microwave region because the scattering cross section is inversely proportional to the fourth power of the wavelength.

g) Terrestrial Magnetic Fields

Because the Faraday rotation switch (FRS) is magnetically controlled, perturbations in the switching field caused by local fields can be a problem. From knowledge of the switch coil geometry and winding, the switch field is approximately H = 9.2 G. Measurements of the local environment at Berkeley with a Hall probe magnetometer show the local field is essentially that of the earth's with the a total magnitude $0.5 \pm 0.1\ G$ in agreement with USGS map showing $|B| = 0.51$ G. Because the ferrite in the FRS has a magnetization dependent absorption, any external magnetic field combined with a misalignment of the ferrite about the physical rotation axis of the equipment could cause a signal. For this reason the FRS was magnetically shielded with several layers of 4 mil mu-metal foil. Measurements show that a single layer of mu-metal reduces transverse fields by a factor of 10^2 and longitudinal fields by a factor of 10. Tests with a Helmholtz pair of coils (separation equals radius) along three axes at fields up to 10 G show that the induced signal caused by the earth is less than 0.08 mK at the 95% confidence level.

h) Depolarization Processes

Consideration must be given to processes which could reduce or depolarize an initially polarized signal.

Since a plasma in a magnetic field becomes birefringent, a plasma in a turbulent magnetic field could be a possible source of depolarization tending to randomly rotate the polarization vector. Table 4 lists the rotation expected from various sources at our frequency. With the exception of an ionized dense universe and a global magnetic field, all known effects are small.

An interesting geometrical depolarizing effect has been suggested by Brans (1975). In this case, an axisymmetric universe causes a scrambling of polarization due to the changing geometry of the universe. This effect has been shown to be small for "reasonable" models of the universes (Caderni *et al.*, 1978b).

Table 4. Possible sources of Faraday rotation and depolarization of the cosmic background radiation.

FARADAY ROTATION & DEPOLARIZATION

Plane of polarization rotated by $\Delta\phi \simeq 81\,\lambda^2 \int N(r)B(r)\cos\theta(r)dr$

λ — cm
N — cm^{-3} e^- density
B — gauss
θ — angle between $\bar{B}$ and direction of propagation.
r — pc 1 pc ~ 3.1×10^{18} cm ~ 3.3 ly

$\Delta\phi \simeq 70\,NB\,r$ $\lambda = 0.91$ cm

Source	N cm^{-3}	B g	r pc	$\Delta\phi$ rad
Galaxy	10^{-3}	10^{-5}	10^{4}	$< 10^{-2}$
Ionosphere	10^{6}	1	10^{-11}	$< 10^{-3}$
Extragalactic[1]	10^{-5}	B	10^{10}	$\lesssim 10^{7}$ B
Extragalactic[2]	10^{-9}	B	10^{10}	$\lesssim 10^{3}$ B
Solar wind	1	10^{-4}	10^{-3}	$< 10^{-5}$

1 Assuming complete ionization in a critically dense universe with a universal magnetic field B.

2. As in 1 except ionized fraction = 10^{-4}.

5. MEASURED DATA AND FITTED PARAMETERS

a) Measured Data

Table 5 gives a list of the data and errors at each declination surveyed. These data have been corrected for the temperature dependence of the Faraday rotation switch and for the instrument wobble in runs where the apparatus was not pointed vertically. The northern hemisphere data consist of several runs at each declination which have been merged. Figure 9 shows the data in graphical form at each declination. Because of the restrictions imposed by contamination from the sun and the limited time in the southern hemisphere, the errors are not equal for each declination. The quoted errors are actual rms errors, based on the scatter of repeated measurements.

b) Spherical Harmonic Fits

A least-squares fit to various spherical harmonics is made using the binned hourly data presented in Table 5. The fitting functions, amplitudes, and errors are shown in Table 6. Independent fits are made to the average, dipole, quadrupole, and octupole spherical harmonics. None of the fitted coefficients is very significant.

A fit to the null hypothesis (no polarization) yields a chi-squared of 279 with 264 degrees of freedom and a corresponding confidence level of 25% for Q and a chi-squared of 265 with 264 degrees of freedom and a confidence level of 47% for U. In addition, the model of Rees gives a definite prediction as to the functional form of Q and U for a model of anisotropic expansion with a given axis of symmetry (Nanos, 1979). Table 7 summarizes the best fit to this model. While the model produces a fairly good fit to the data, it is not significant. *We have found no evidence for linear polarization over any of the areas surveyed.*

c) Comparison to Previous Measurements

There have been two previous measurements of the polarization of the cosmic

Table 5. List of all data and errors at each declination by hour in siderial time after correction for ferrite temperature and instrument wobble.

DECLINATION	R.A.	Q	SIGMA Q	U	SIGMA U
-37.00	.50	.69	.61	.72	.53
-37.00	1.50	1.22	.53	.19	.58
-37.00	2.50	.10	.74	.88	.86
-37.00	3.50	-.08	.71	-.06	.79
-37.00	4.50	.23	.80	.25	.75
-37.00	5.50	.38	.60	1.67	.87
-37.00	6.50	-.32	.68	.47	.70
-37.00	7.50	-.12	.83	-.70	.93
-37.00	8.50	-.29	.62	.20	.74
-37.00	9.50	-.33	.74	-.48	.85
-37.00	10.50	-.17	.91	.97	.96
-37.00	11.50	-1.27	.94	-.11	.71
-37.00	12.50	.61	1.02	-.20	.90
-37.00	13.50	-1.11	.81	-.28	.68
-37.00	14.50	.14	1.05	.18	.89
-37.00	15.50	-1.81	.87	.23	.96
-37.00	16.50	-1.69	.87	-.86	1.08
-37.00	17.50	-.03	.80	-.13	1.14
-37.00	18.50	1.29	.81	.90	.66
-37.00	19.50	-1.00	.80	-1.21	.79
-37.00	20.50	1.00	.63	.12	.64
-37.00	21.50	.13	.57	-1.45	.63
-37.00	22.50	.63	.56	-.47	.52
-37.00	23.50	.47	.49	-.47	.49
-20.00	.50	-1.16	1.52	-.23	1.20
-20.00	1.50	.64	.71	.55	.99
-20.00	2.50	1.14	1.23	-.08	1.33
-20.00	3.50	-1.03	1.22	2.61	1.36
-20.00	4.50	-1.34	1.03	-2.52	1.56
-20.00	5.50	-.90	1.68	1.37	1.22
-20.00	6.50	1.35	1.75	.67	1.89
-20.00	7.50	.01	1.40	.23	1.12
-20.00	8.50	1.56	1.51	1.95	1.04
-20.00	9.50	.14	.93	-2.09	1.20
-20.00	10.50	.84	1.21	-.58	.96
-20.00	11.50	-1.82	2.06	-.28	1.11
-20.00	12.50	-.27	1.37	-.43	1.00
-20.00	13.50	3.07	1.89	-1.53	1.63
-20.00	14.50	-1.61	1.60	1.09	1.22
-20.00	15.50	.94	1.83	-1.66	2.71
-20.00	16.50	.54	2.34	-3.11	2.94
-20.00	17.50	1.92	2.00	1.53	1.99
-20.00	18.50	.87	1.36	.35	1.58
-20.00	19.50	-.86	.87	2.05	.97
-20.00	20.50	1.07	1.32	.05	.87
-20.00	21.50	-1.13	.99	-.61	.85
-20.00	22.50	-1.41	1.96	-.43	1.83
-20.00	23.50	.31	1.48	1.62	1.30

Table 5 cont.

DECLINATION	R.A.	Q	SIGMA Q	U	SIGMA U
13.00	.50	.72	.52	.81	.52
13.00	1.50	-.88	.56	-.28	.56
13.00	2.50	.07	.57	-.43	.57
13.00	3.50	-.13	.57	.71	.57
13.00	4.50	-.69	.59	1.15	.57
13.00	5.50	1.14	.65	.10	.65
13.00	6.50	-.30	.50	.72	.64
13.00	7.50	.71	.56	.60	.57
13.00	8.50	.35	.49	-.17	.60
13.00	9.50	.08	.59	.31	.49
13.00	10.50	-.21	.66	.13	.55
13.00	11.50	.35	.65	.28	.51
13.00	12.50	.17	.61	-1.10	.72
13.00	13.50	.06	.71	.08	.73
13.00	14.50	-.65	.69	-1.61	.61
13.00	15.50	-.36	.64	-.19	.77
13.00	16.50	-.99	.64	.06	.83
13.00	17.50	-.36	.67	-.19	.69
13.00	18.50	1.12	.61	.25	.64
13.00	19.50	.93	.61	-1.01	.74
13.00	20.50	-.46	.65	.37	.57
13.00	21.50	.98	.57	.17	.68
13.00	22.50	1.17	.63	-.75	.58
13.00	23.50	-.74	.54	.53	.57
18.00	.50	-.39	.46	-.03	.50
18.00	1.50	-.67	.57	.70	.46
18.00	2.50	.49	.56	-.43	.55
18.00	3.50	.64	.44	.13	.48
18.00	4.50	.02	.55	-.32	.50
18.00	5.50	.35	.51	-.05	.49
18.00	6.50	-.07	.63	.85	.55
18.00	7.50	-.36	.59	-.19	.65
18.00	8.50	.02	.44	-.26	.54
18.00	9.50	-.22	.57	.51	.48
18.00	10.50	-.31	.55	-.27	.48
18.00	11.50	.37	.51	-.63	.50
18.00	12.50	1.00	.52	.55	.62
18.00	13.50	-1.05	.49	-.78	.53
18.00	14.50	.60	.45	-.12	.41
18.00	15.50	-.48	.50	1.74	.50
18.00	16.50	.02	.46	-.54	.48
18.00	17.50	-.29	.53	.63	.49
18.00	18.50	-.53	.49	-.09	.46
18.00	19.50	-.11	.55	-.18	.42
18.00	20.50	-.60	.61	-.52	.61
18.00	21.50	.30	.48	-.49	.48
18.00	22.50	-.07	.49	.14	.52
18.00	23.50	-.28	.47	-.47	.54

Table 5 cont.

DECLINATION	R.A.	Q	SIGMA Q	U	SIGMA U
23.00	.50	.28	.50	.65	.57
23.00	1.50	-.64	.47	.31	.53
23.00	2.50	.01	.46	.15	.46
23.00	3.50	-.35	.49	.15	.43
23.00	4.50	.01	.49	-.25	.45
23.00	5.50	.84	.42	-.38	.50
23.00	6.50	.48	.54	.76	.48
23.00	7.50	.33	.52	.39	.48
23.00	8.50	-.26	.60	.24	.55
23.00	9.50	.80	.59	-.37	.35
23.00	10.50	.15	.50	-.29	.61
23.00	11.50	.30	.39	-.32	.52
23.00	12.50	.47	.50	.10	.53
23.00	13.50	.66	.40	.26	.42
23.00	14.50	-.34	.48	.14	.42
23.00	15.50	-.40	.43	-.46	.47
23.00	16.50	-.70	.50	.06	.59
23.00	17.50	.35	.49	-.02	.50
23.00	18.50	-.38	.43	.12	.50
23.00	19.50	-1.55	.38	-.41	.50
23.00	20.50	.37	.55	-.07	.42
23.00	21.50	.05	.58	.53	.48
23.00	22.50	.59	.43	-1.01	.51
23.00	23.50	.19	.45	.63	.39
28.00	.50	.74	.56	-.53	.53
28.00	1.50	.73	.40	.22	.50
28.00	2.50	-.58	.48	-.15	.45
28.00	3.50	-.40	.54	-.33	.40
28.00	4.50	-.30	.59	-.69	.52
28.00	5.50	.12	.45	.46	.42
28.00	6.50	.10	.45	.39	.49
28.00	7.50	-.26	.42	.32	.48
28.00	8.50	-1.11	.38	-.70	.47
28.00	9.50	.05	.52	.25	.45
28.00	10.50	.01	.56	.02	.50
28.00	11.50	1.08	.54	-.12	.45
28.00	12.50	-1.00	.43	.52	.52
28.00	13.50	-.22	.48	-.61	.50
28.00	14.50	.08	.39	.33	.45
28.00	15.50	-.50	.48	-.05	.52
28.00	16.50	-.15	.48	.15	.49
28.00	17.50	-.09	.40	.37	.53
28.00	18.50	.75	.38	-.22	.55
28.00	19.50	-.00	.50	.01	.46
28.00	20.50	-.57	.46	.28	.47
28.00	21.50	.30	.55	-.49	.46
28.00	22.50	-.13	.45	-1.76	.57
28.00	23.50	.37	.51	.07	.53

Table 5 cont.

DECLINATION	R.A.	Q	SIGMA Q	U	SIGMA U
38.00	.50	.27	.30	.03	.32
38.00	1.50	-.19	.29	.45	.35
38.00	2.50	.10	.31	.17	.30
38.00	3.50	-.53	.30	.25	.33
38.00	4.50	-.25	.37	-.42	.32
38.00	5.50	-.10	.32	.37	.32
38.00	6.50	.11	.37	-.01	.32
38.00	7.50	.07	.32	.21	.36
38.00	8.50	.19	.30	.03	.32
38.00	9.50	-.20	.32	.39	.33
38.00	10.50	.25	.30	-.16	.32
38.00	11.50	-.49	.30	-.11	.30
38.00	12.50	-.02	.30	.37	.33
38.00	13.50	.03	.28	.05	.27
38.00	14.50	.04	.30	.19	.29
38.00	15.50	.12	.33	.09	.29
38.00	16.50	-.22	.31	-.30	.32
38.00	17.50	.54	.31	-.67	.27
38.00	18.50	.03	.29	-.09	.30
38.00	19.50	.18	.31	.14	.31
38.00	20.50	-.18	.30	.43	.26
38.00	21.50	.17	.31	.41	.27
38.00	22.50	.34	.33	-.60	.28
38.00	23.50	-.08	.32	-.20	.27
48.00	.50	-.15	.42	-.42	.41
48.00	1.50	-.51	.49	.21	.51
48.00	2.50	-.00	.42	-.39	.49
48.00	3.50	-.63	.52	.49	.48
48.00	4.50	-.33	.47	.13	.44
48.00	5.50	.57	.44	-.44	.43
48.00	6.50	-.09	.50	-.20	.44
48.00	7.50	-.10	.46	-.58	.49
48.00	8.50	-.02	.46	.08	.48
48.00	9.50	.24	.39	.23	.43
48.00	10.50	.44	.47	-.38	.53
48.00	11.50	-.07	.42	.03	.42
48.00	12.50	.57	.49	-.26	.49
48.00	13.50	-1.22	.60	-.41	.46
48.00	14.50	.29	.40	.25	.45
48.00	15.50	-.47	.33	.35	.43
48.00	16.50	-.18	.43	.15	.42
48.00	17.50	.08	.47	.84	.52
48.00	18.50	1.06	.39	-.20	.47
48.00	19.50	-.37	.42	-.56	.43
48.00	20.50	.13	.38	.14	.48
48.00	21.50	.75	.48	.75	.47
48.00	22.50	-.30	.42	-.37	.49
48.00	23.50	-.27	.39	.13	.48

Table 5 cont.

DECLINATION	R.A.	Q	SIGMA Q	U	SIGMA U
53.00	.50	.77	.32	.37	.30
53.00	1.50	-.04	.31	.22	.30
53.00	2.50	-.56	.29	-.13	.31
53.00	3.50	.16	.34	.66	.33
53.00	4.50	-.39	.32	.05	.32
53.00	5.50	-.26	.36	.09	.28
53.00	6.50	.17	.30	-.14	.35
53.00	7.50	.17	.30	-.26	.30
53.00	8.50	-.44	.31	-.26	.31
53.00	9.50	-.48	.28	-.39	.30
53.00	10.50	-.32	.25	-.10	.26
53.00	11.50	.22	.31	.04	.35
53.00	12.50	-.18	.30	-.16	.34
53.00	13.50	.04	.32	-.06	.30
53.00	14.50	-.31	.29	-.46	.28
53.00	15.50	.17	.30	.78	.30
53.00	16.50	.32	.32	-.08	.28
53.00	17.50	-.24	.32	-.18	.33
53.00	18.50	-.20	.32	-.41	.30
53.00	19.50	-.49	.29	-.49	.30
53.00	20.50	.56	.30	-.07	.34
53.00	21.50	.32	.30	-.10	.32
53.00	22.50	-.27	.32	-.34	.32
53.00	23.50	-.22	.31	.15	.32
58.00	.50	.27	.46	-.18	.44
58.00	1.50	-.61	.41	.47	.43
58.00	2.50	.54	.48	-.67	.50
58.00	3.50	-.40	.44	-.30	.45
58.00	4.50	.30	.40	.22	.40
58.00	5.50	-.22	.38	-.88	.39
58.00	6.50	.29	.43	.16	.40
58.00	7.50	-.65	.42	-.45	.41
58.00	8.50	.02	.42	.05	.40
58.00	9.50	.05	.41	.04	.40
58.00	10.50	.43	.37	-.68	.38
58.00	11.50	.16	.43	.37	.47
58.00	12.50	.19	.40	.11	.39
58.00	13.50	.52	.33	-.37	.37
58.00	14.50	-.05	.37	.26	.37
58.00	15.50	.30	.36	-.08	.37
58.00	16.50	-.36	.43	.18	.35
58.00	17.50	.45	.39	-.17	.39
58.00	18.50	.25	.37	-.65	.37
58.00	19.50	-.66	.41	.66	.45
58.00	20.50	-.20	.37	-.10	.41
58.00	21.50	.30	.38	-.44	.37
58.00	22.50	-.28	.41	.33	.41
58.00	23.50	-.51	.44	.32	.36

Table 5 cont.

DECLINATION	R.A.	Q	SIGMA Q	U	SIGMA U
63.00	.50	-.60	.39	-.08	.36
63.00	1.50	.10	.41	.35	.38
63.00	2.50	.01	.37	.21	.38
63.00	3.50	-.01	.34	.14	.35
63.00	4.50	.03	.38	-.23	.33
63.00	5.50	-.07	.40	.40	.33
63.00	6.50	-.12	.32	-.04	.37
63.00	7.50	-.14	.28	-.01	.34
63.00	8.50	.16	.32	.13	.38
63.00	9.50	.63	.36	.23	.34
63.00	10.50	.40	.32	-.07	.36
63.00	11.50	.16	.34	.15	.35
63.00	12.50	.36	.33	-.07	.39
63.00	13.50	.05	.32	-.57	.34
63.00	14.50	-.17	.36	.33	.36
63.00	15.50	-.00	.37	-.10	.32
63.00	16.50	.05	.39	1.34	.34
63.00	17.50	-.19	.38	-.39	.36
63.00	18.50	-.39	.34	-.17	.38
63.00	19.50	-.06	.39	-.05	.36
63.00	20.50	-.43	.39	.10	.36
63.00	21.50	.30	.35	-.14	.37
63.00	22.50	-.04	.39	-.52	.41
63.00	23.50	.76	.42	-.19	.43

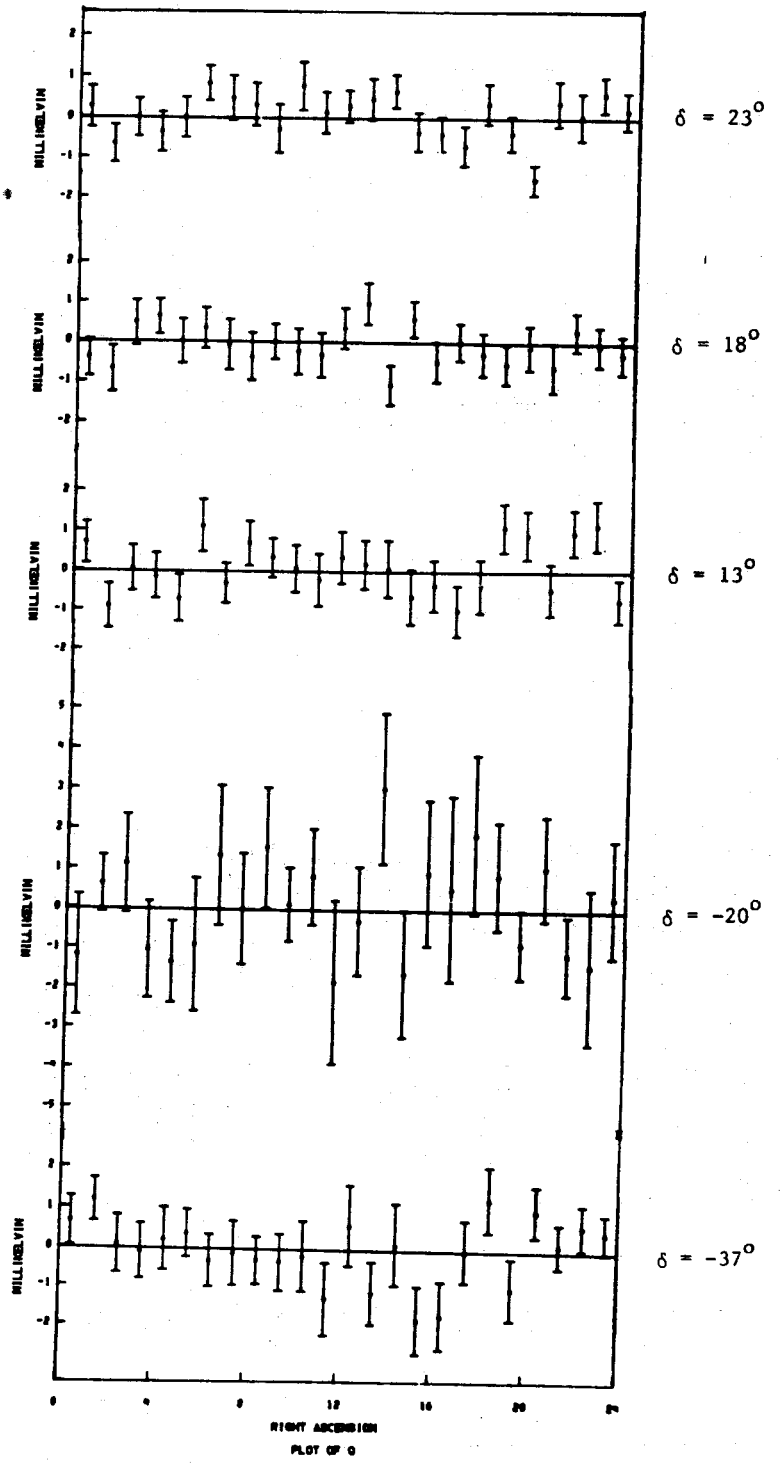

XBL 802-8412

Figure 9. Data for each declination surveyed plotted in hourly bins by siderial time.

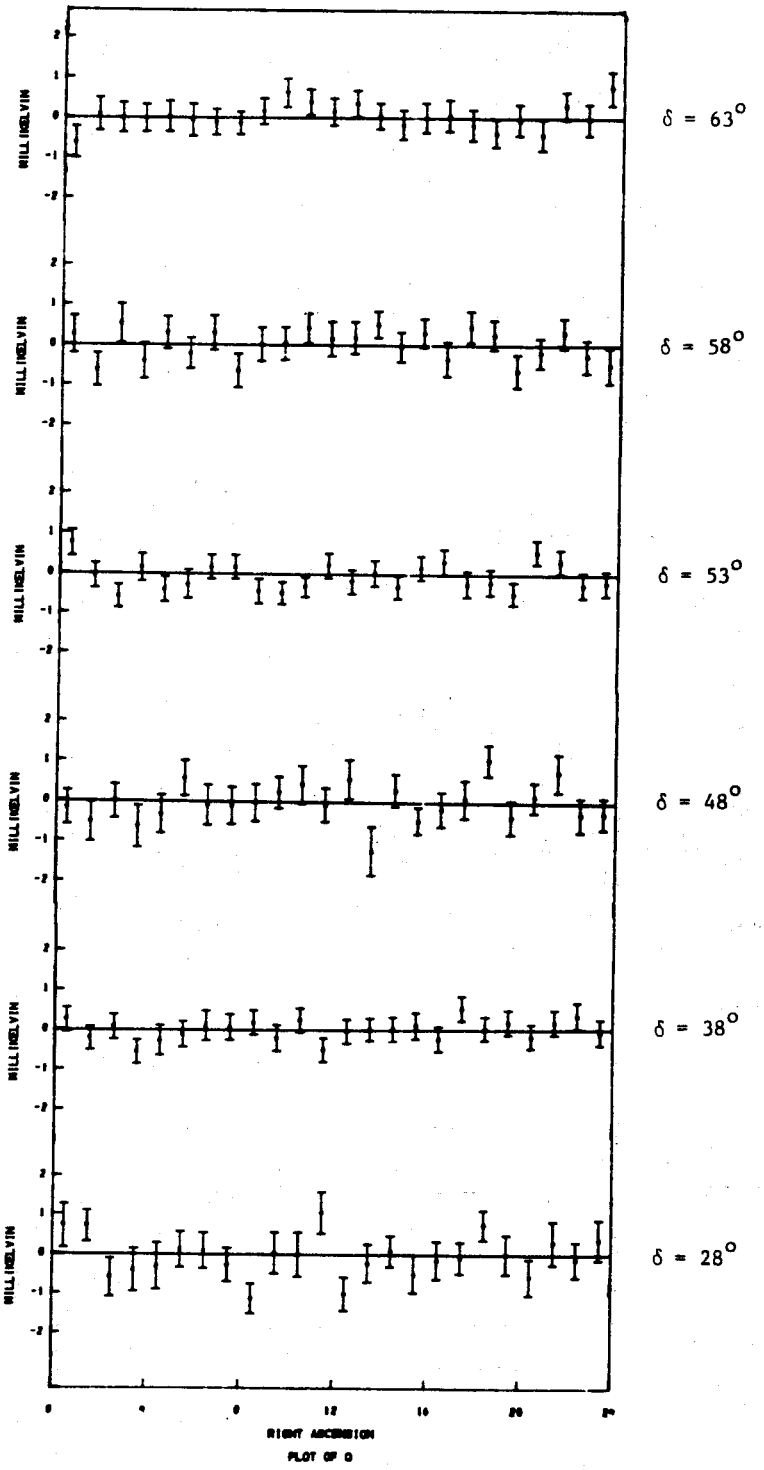

XBL 802-8409

Figure 9 cont.

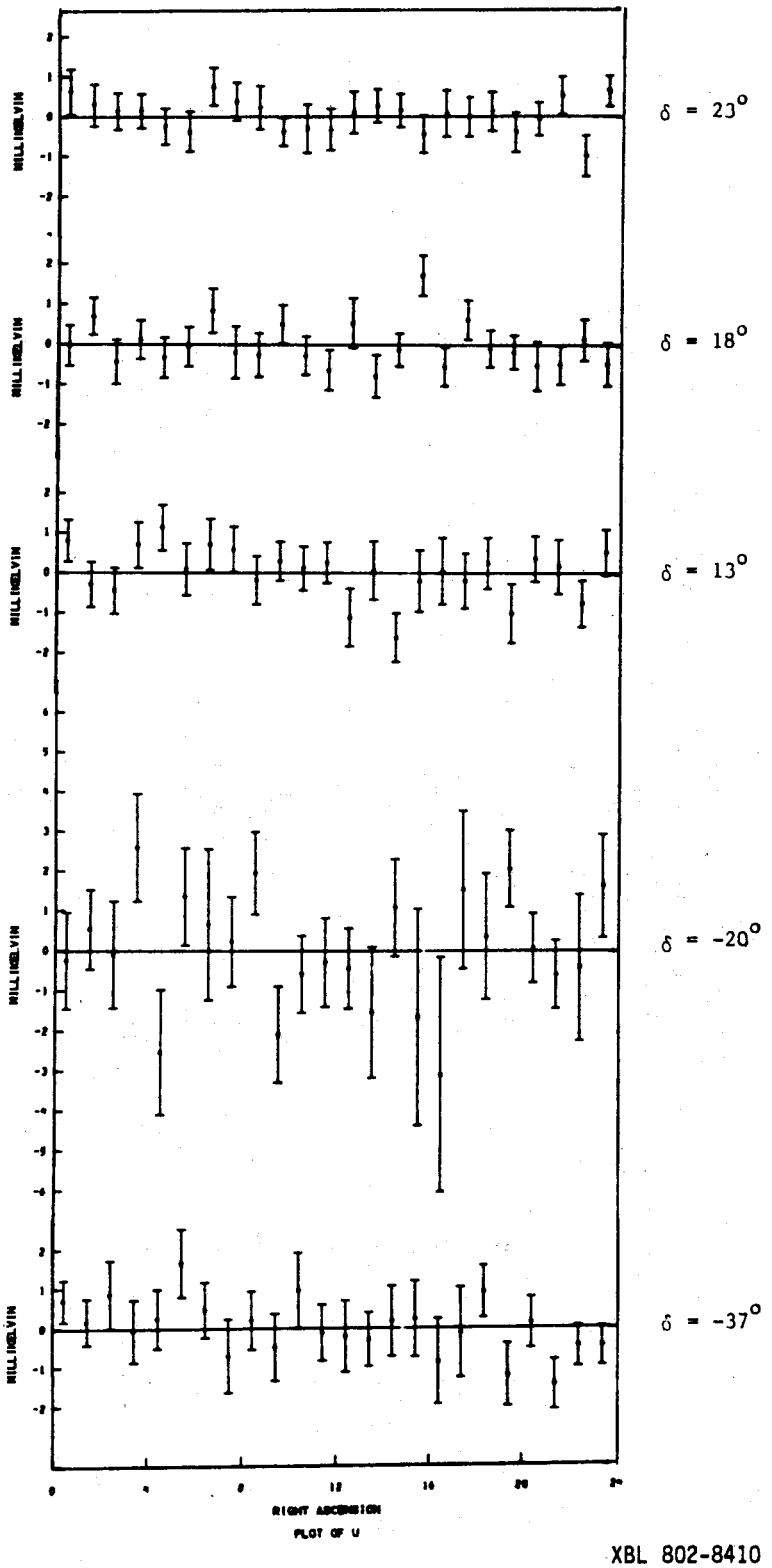

Figure 9 cont.

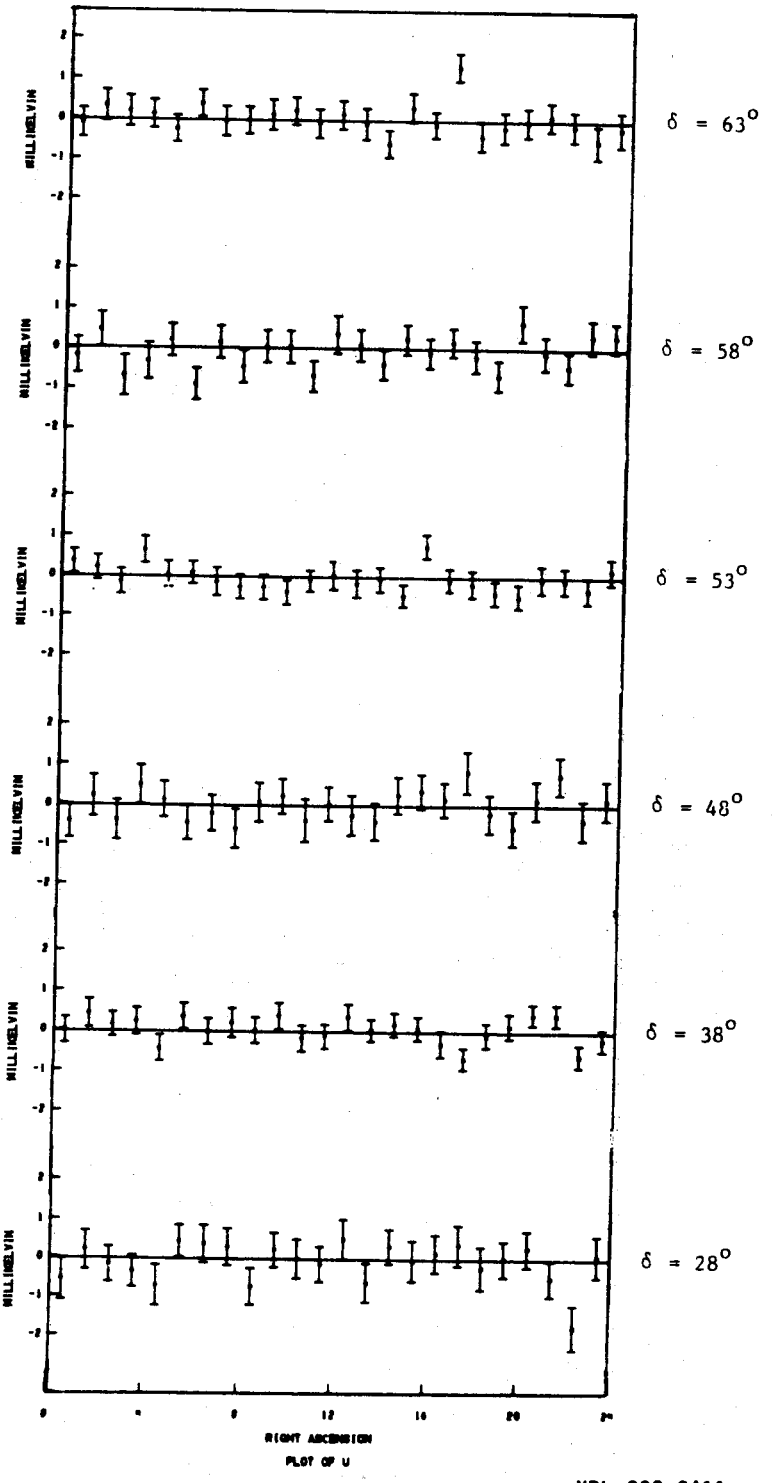

XBL 802-8411

Figure 9 cont.

Table 6
Spherical Harmonic Fits - Independent Fits
milli-Kelvin

Fitting Function P_l^m	Q Fit	U Fit	Error
1	0.00	-0.01	0.03
$\sin\delta$	-0.02	-0.03	0.04
$\cos\delta\cos\alpha$	0.02	0.02	0.05
$\cos\delta\sin\alpha$	0.00	0.08	0.05
$\frac{1}{2}(3\sin^2\delta-1)$	-0.02	-0.05	0.06
$\cos2\delta\cos\alpha$	-0.05	0.01	0.04
$\cos2\delta\sin\alpha$	-0.03	0.02	0.04
$\cos^2\delta\cos2\alpha$	0.08	-0.06	0.06
$\cos^2\delta\sin2\alpha$	-0.10	0.15	0.06
$\frac{1}{2}(5\sin^3\delta-3\sin\delta)$	0.04	-0.03	0.08
$\frac{1}{4}\cos\delta(5\sin^2\delta-1)\cos\alpha$	-0.02	0.01	0.05
$\frac{1}{4}\cos\delta(5\sin^2\delta-1)\sin\alpha$	-0.06	0.01	0.05
$\cos2\delta\sin\delta\cos2\alpha$	0.03	0.01	0.05
$\cos2\delta\sin\delta\sin2\alpha$	-0.05	0.08	0.05
$\cos^3\delta\cos3\alpha$	-0.01	0.06	0.07
$\cos^3\delta\sin3\alpha$	-0.07	0.04	0.08

Fit	Q: $\frac{\chi^2}{DOF}$	U: $\frac{\chi^2}{DOF}$
1	279/263 CL=24%	279/263 CL=24%
Dipole	279/261 CL=21%	281/261 CL=19%
Quadrupole	274/259 CL=25%	296/259 CL= 6%

background radiation, Nanos (1979) and Caderni *et al.* (1978a); both with null results. Nanos performed a polarization experiment similar to this one in 1973 at a wavelength of 32 mm for one declination of $\delta = 40°$. Caderni *et al.* used a balloon-borne infrared spectrometer operating at a wavelength of 0.5 - 3 mm, but were forced to terminate after only four hours of data taking. Because of the limited sky coverage in both experiments, these data were not fit to spherical harmonics. The results of Nanos and Caderni *et al.* are summarized in Table 8. Although Nanos' data shows a significant (5σ) average value for Q and U, this was interpreted as sidelobe pickup from a nearby building. The work described here represents about an order of magnitude improvement over previous measurements.

Table 7
Fit to Anisotropic Axisymmetric Model (Rees)

Prediction of Model

$$Q = (T_w - T_a)_{max}\,[\cos^2\delta(1 - 3/2\sin^2\theta_0)$$
$$+ \sin 2\theta_0 \cos\delta \sin\delta \sin(t - \alpha_0 - \pi/2)$$
$$+ \sin^2\theta_0(1 - 1/2\cos^2\delta)\sin 2(t - \alpha_0 + \pi/4)]$$

$$U = -(T_w - T_a)_{max}[\sin 2\theta_0 \cos\delta \sin(t - \alpha_0 + \pi)$$
$$+ \sin^2\theta_0 \sin\delta \sin 2(t - \alpha_0)]$$

θ_0 - angle from celestial pole to symmetry axis of universe

α_0 - right ascension of symmetry axis of universe

Least Squares Fit to model gives :

$$(T_w - T_a)_{max} = -0.07 \pm 0.04\ mK$$

$$\theta_0 = 40 \pm 20^o$$

$$\alpha_0 = 13 \pm 1.5\ hr$$

$$\frac{\chi^2}{DOF} = \frac{542}{525}$$

CL = 30 %

Table 8

Results of Previous Measurements

Nanos (1979)

$\delta = 40^o$ 15^o beam width $\lambda = 32$ mm

Period	Q Fit	U Fit	Error
Average	-0.67	-0.88	0.14
24 hr	0.52	0.58	0.20
12 hr	0.20	0.45	0.20

milli-Kelvin

Fit to anisotropic model of Rees (1968) yields 1.6 mK 90% C.L. limit

Caderni et al. (1978)

δ -10^o to -45^o

α = 17.5 to 20.5 hrs.

Q , U < 2 mK 70% confidence level over area covered

Data base too small to fit to functional forms

6. ASTROPHYSICAL INTERPRETATION

a) Limits on Anisotropic Models

The polarization limits obtained in this experiment can be used to set limits on the types of models useful in describing the universe, as well as physical processes which can occur. In general, any model which produces an intrinsic intensity anisotropy in the background radiation will also produce a polarization. Intrinsic anisotropy refers to that which is not produced by our own particular frame of reference and which is present prior to the time of decoupling. Examples of intrinsic anisotropies include rotation of the universe and anisotropic expansion. Examples of anisotropies which are *not* intrinsic include local inhomogeneities (masses), local gravity waves, and the motion of our galaxy. These latter anisotropies would not be expected to produce any polarization. As stated before one advantage of this experiment is that it is only sensitive to intrinsic anisotropies; any perturbations present in the intensity which are simply due to our peculiar reference frame do not produce a polarization and thus need not be subtracted away.

The degree of polarization induced by a given intrinsic anisotropy depends on the time at which decoupling occurred, since this sets the time scale on which matter and radiation interact. More specifically, the polarization depends on the ionization fraction as a function of time. Two cases will be considered in this regard. In case I, decoupling occurs at a Z of 1500 with no reionization at later times. In case II, decoupling occurs at a Z of 1500, but matter is later reionized at a Z of 7, possibly corresponding to the era of early galaxy formation. In both cases, the calculations of Peebles (1968) are used for the ionization fraction through the era of decoupling (Negroponte and Silk, 1980 ; Basko and Polnorev, 1980) and critical density is assumed. Table 9 gives the limits that the polarization measurement places on two processes in terms of the cases mentioned.

The calculations of Negroponte and Silk (1980) are used for the limits on anisotropic expansion and large scale density fluctuations.

Table 9
Model Constraints From Polarization Data

Model	Case 1 (no reionization)	Case 2 (reionization z=7)
Anisotropic Expansion	$\frac{\delta h_0}{h_0} < 6\times10^{-8}$	$\frac{\delta h_0}{h_0} < 2\times10^{-8}$
Density Fluctuations (Large Scale)	$\frac{\delta\rho_0}{\rho_0} < 1$	$\frac{\delta\rho_0}{\rho_0} < 2\times10^{-3}$

b) Comparison to Intensity Measurements

The best limits on the intensity anisotropy other than the first order (motion) anisotropy come from the Princeton and Berkeley anisotropy experiments. The measured value of the first order term and limits on the higher order terms are shown in Table 10.

Table 10
Comparison To Intensity Measurements

Dipole and Quadrupole Fit - mK

	Intensity*		Polarization		
Fitting Function	Fit	Error	Q Fit	U Fit	Error
$\sin\delta$	-0.18	0.39	-0.02	-0.03	0.04
$\cos\delta\cos\alpha$	-2.78	0.28	0.02	0.02	0.05
$\cos\delta\sin\alpha$	0.66	0.29	0.00	0.08	0.05
$\frac{1}{2}(3\sin^2\delta-1)$	0.38	0.26	-0.02	-0.05	0.06
$\sin2\delta\cos\alpha$	-0.34	0.29	-0.05	0.01	0.04
$\sin2\delta\sin\alpha$	0.02	0.24	-0.03	0.02	0.04
$\cos^2\delta\cos2\alpha$	-0.11	0.16	0.08	-0.06	0.06
$\cos^2\delta\sin2\alpha$	0.06	0.20	-0.10	0.15	0.06

*(Smoot and Lubin 1979)

A direct comparison between polarization and intensity is not possible without a model to connect these two intrinsically different processes. A comparison between polarization and intensity measurements is given in Table 11 for the case of an axisymmetric, anisotropic universe, based on the model of Rees (1968) and the calculations of Negroponte and Silk (1980).

c) Quadrupole Measurement

Table 11
Comparison of Polarization and Intensity

Case	$\frac{P}{\epsilon}$ = ratio of pol. to int.
No reheat of plasma	0.04
Reheat at z = 7	
Ω_H=1	0.3
Ω_H=0.1	0.07
Reheat at z = 40 Ω_H=1	2
Reheat at z = 100 Ω_H=1	0.5

Fabbri *et al.* (1980) have recently reported the existence of a possible quadrupole component in the cosmic background radiation with an amplitude of about 1 mK. Their measurements are taken near the peak (0.5 - 3 *mm*), and are not directly comparable to our polarization data or past isotropy data for two reasons. One, if the spectrum is distorted near the peak as reported by Woody and Richards (1979) then both the dipole and quadrupole amplitude will differ from the lower frequency values (Lubin, 1980b). Secondly, because the data of Fabbri *et al.* have limited sky coverage, the precise functional form of the anisotropy is not well established. However, if we assume the spectrum is Plankian (blackbody), then the calculations of Negroponte and Silk (1980) indicate that to measure a polarization resulting from the reported anisotropy at our level of sensitivity, the intergalactic medium would need to be near critical density and that there be a significant reionization by a red shift $Z > 7$ for us to see a positive effect at our 0.3 mK 95% confidence level upper limit.

ACKNOWLEDGEMENTS

This work was supported by the National Aeronautics and Space Adminstration and by the High Energy Physics Research Division of the U.S. Department of Energy under contract No. W-7405-ENG-48. The California Space Group is supporting a portion of the continuation of this work under grant No. 539579-20533.

We gratefully acknowledge the contribution of C. Witebsky for his assistance with estimates of galactic background. This work would not have been possible without the diligent efforts of our staff J.S. Aymong, H. Dougherty, J. Gibson, and N. Gusack and without the assistance and encouragement of our colleagues S. Friedman, S. Peterson, and C. Witebsky.

References

Basko, M.M. and Polnarev, A.G. 1980, *Monthly Notices of Royal Astronomical Society* **191** , 207.

Berkhuijsen, E. M. 1971, *Astron. Astrophys.* **14** , 359.

Berkhuijsen, E. M. 1972, *Astron. Astrophys. Suppl.* **5** , 263.

Brans, C. H. 1975, *Ap. J.* **197** , 1.

Brouw, W. N. and Spoelstra, T. A. Th. 1976, *Astron. Astrophys. Suppl.* **26** , 129.

Caderni, N., Fabbri, R., Melchiorri, B., Melchiorri, F. and Natale, V. 1978a, *Phys. Rev.* **D17** , 8, 1908.

Caderni, N., Fabbri, R., Melchiorri, B., Melchiorri, F. and Natale, V. 1978b, *Phys. Rev.* **D17** , 8, 1901.

Cheng, E. S., Saulson, P. R., Wilkinson, D. T. and Corey, B. E. 1979, *Ap. J. Lett.* **232** , L139.

Chu, T. S., Gans, M. J. and Legg, W. E. 1975, *Bell. Sys. Tech. J.* **54** , 10, 1665.

Collins, C. B. and Hawking, S. W. 1973, *Mon. Not. R. Astr. Soc.* **162** , 307.

Corey, B. E. and Wilkinson, D. T. 1976, *Bull. Am. Astro. Soc.* **8** 351.

Fabbri, R., Guidi, I., Mechiorri, F., and Natale, V. 1980, *Phys. Rev. Lett.* **44, 23.**

Gorenstein, M. V. and Smoot, G. F., *Ap. J.* to be published 1980.

Harrison, E. R. 1973, *Ann. Rev. Astron. Astrophys.* , **11, 155**

Hawking, S. 1969, *Mon. Not. R. Astr. Soc.* **142** , 129.

Kraus, J. D. 1966, *Radio Astronomy* (McGraw-Hill).

Lubin, P. M. and Smoot, G. F. 1979, *Phys. Rev. Lett.* **42** , 2, 129.

Lubin, P.M., *Ph.D. Thesis* U.C. Berkeley, 1980a , L.B.L. report # 10934.

Lubin, P.M., Internal group memo, unpublished, NASA note number 411, 1980b.

Mach, E. 1893, *The Science of Mechanics (2nd ed. Open Court Publishing Co.).*

Nanos, G. P. 1974, *Ph.D. Thesis* , Princeton University.

Nanos, G. P. 1979, *Ap. J.* **232** , 341.

Negroponte, J. and Silk, J. 1980 *Phys. Rev. Lett.* **44**, 1433.

Owens, D. K., Muehlner, D. J. and Weiss, R. 1979, *Ap. J.* **231** , 702.

Peebles, P. J. E. 1968, *Ap. J.* **153** , 11.

Penzias, A. A. and Wilson, R. W. 1965, *Ap. J.* **142** , 419.

Rees, M. J. 1968, *Ap. J. Lett.* **153** , L1.

Shurcliff, W. A. and Ballard, S. S. 1962, *Polarized Light (D. Van Nostrand Co.: N.J.).*

Smoot, G. F., Gorenstein, M. V. and Muller, R. A. 1977, *Phys. Rev. Lett.* **39** , 14, 898.

Smoot, G. F. and Lubin, P. M. 1979, *Ap. J. Lett.* **234** , L117.

Weinberg, S. 1972, *Gravitation and Cosmology: Principles and Applications of the General Theory of Relativity* (John Wiley and Sons: N.Y.).

Witebsky, C. 1978, Internal group memo, unpublished, NASA note number 361.

Woody, D. P. and Richards, P. L. 1979, *Phys. Rev. Lett.* **42** , 14 925.